www.czasopisma.pan.pl PAN POLSKA AKADEMIA NAUK www.journals.pan.pl

A R C H I V E S O F M E T A L L U R G Y A N D M A T E R I A L S

Volume 60 2015 Issue 1

DOI: 10.1515/amm-2015-0010

T. LIPIŃSKI*, A. WACH*

THE EFFECT OF FINE NON-METALLIC INCLUSIONS ON THE FATIGUE STRENGTH OF STRUCTURAL STEEL

WPŁYW DROBNYCH WTRĄCEŃ NIEMETALICZNYCH NA WYTRZYMAŁOŚĆ ZMĘCZENIOWĄ STALI KONSTRUKCYJNEJ

The article discusses the results of a study investigating the effect of the number of fine non-metallic inclusions (up to 2 μm in size) on the fatigue strength of structural steel during rotary bending. The study was performed on 21 heats produced in an industrial plant. Fourteen heats were produced in 140 ton electric furnaces, and 7 heats were performed in a 100 ton oxygen converter. All heats were desulfurized. Seven heats from electrical furnaces were refined with argon, and heats from the converter were subjected to vacuum circulation degassing.

Steel sections with a diameter of 18 mm were hardened and tempered at a temperature of 200, 300, 400, 500 and 600°C. The experimental variants were compared in view of the applied melting technology and heat treatment options. The results were presented graphically, and the fatigue strength of steel with a varied share of non-metallic inclusions was determined during rotary bending. The results revealed that fatigue strength is determined by the relative volume of fine non-metallic inclusions and tempering temperature.

Keywords: steel, structural steel, non-metallic inclusions, fatigue strength, bending fatigue, bending pendulum

W pracy przedstawiono wyniki badań wpływu ilości drobnych wtrąceń niemetalicznych, o wielkości do 2 μm, na wytrzymałość zmęczeniową przy zginaniu obrotowym. Badania prowadzono na 21 wytopach wyprodukowanych w warunkach przemysłowych. 14 wytopów wykonano w piecach elektrycznych o pojemności 140 ton i 7 wytopów w konwertorze tlenowym o pojemności 100 ton. Wszystkie wytopy poddawano odsiarczaniu. 7 wytopów pochodzących z pieca elektrycznego poddawano rafinacji argonem, zaś wytopy z konwertora odgazowaniu próżniowemu.

Odcinki ze stali o średnicy 18 mm hartowano i odpuszczano w temperaturach: 200, 300, 400, 500 lub 600°C. Warianty badań zestawiono uwzględniając technologię wytapiania stali opcje obróbki cieplnej. Wyniki przedstawiono w graficznej postaci uwzględniającej zależności wytrzymałości zmęczeniowej przy obrotowym zginaniu z udziałem objętościowym wtrąceń niemetalicznych. Wykazano, że wytrzymałość zmęczeniowa zależy od objętości względnej drobnych wtrąceń niemetalicznych, oraz temperatury odpuszczania.

1. Introduction

Many working elements in machines and devices are subjected to varied loads during operation. Loading paths can be random, but also cyclic. Load produces complex stress in a material [1].

The selection of steel types that are optimal for a given application contributes to reliable machine operation. The durability of machine parts subjected to various loads should be analyzed to achieve the above goal. The results can be used to evaluate the influence of technological manufacturing processes on steel properties. The properties of steel are determined by many interconnected factors that influence its microstructure, including chemical composition, manufacturing technology and heat treatment [2-5]. There are also conducted theoretical and numerical simulations that attempts to predict the distribution of intermetallic phases in the crystallization process of steels [6-8].

Non-metallic inclusions are one of the factors that influence the fatigue strength of steel [9-12]. Despite vast progress in manufacturing technologies, non-metallic inclusions have not been completely eliminated from steel [12-14]. Their negative impact on fatigue strength has been widely discussed in the literature [2,15,16], mostly in studies of hard-fatigue steels with low plasticity and inclusions larger than 5 μm. Selected authors have analyzed the purity and fatigue properties of steels with high plasticity [15,16-19]. The effect of fine non-metallic inclusions measuring up to 5 μm on the fatigue strength of steel has not been thoroughly investigated. Hebsur observed that fatigue crack propagation decreased in steels where fine non-metallic inclusions were irregularly distributed [19]. According to [13,14], steels produced with the use of various methods contain mostly non-metallic inclusions of up to 2 μm in size. High-grade steels contain fewer large-sized inclusions. Non-metallic inclusions generally exert a negative effect of fatigue strength [2,4,16,17]. The above indicates that

* UNIVERSITY OF WARMIA AND MAZURY IN OLSZTYN, THE FACULTY OF TECHNICAL SCIENCES DEPARTMENT OF MATERIALS AND MACHINES TECHNOLOGY, ST: OCZAPOWSKIEGO 11, 10-957 OLSZTYN, POLAND

the dimensions of non-metallic inclusions significantly influence a material's fatigue strength.

2. Aim of the study and methods

The objective of this study was to determine the influence of fine non-metallic inclusions (up to 2 μm in size) on the fatigue strength of structural steel with high plasticity.

The tested material comprised steel manufactured in three different metallurgical processes. The resulting heats differed in purity and size of non-metallic inclusions. Heat treatments were selected to produce heats with different microstructure of steel, from hard microstructure of tempered martensite, through sorbitol to the ductile microstructure of spheroidite.

The experimental material consisted of steel products obtained in three metallurgical processes. In the first process, steel was melted in a 140-ton basic arc furnace. The study was performed on 21 heats produced in an industrial plant. The metal was tapped into a ladle, it was desulfurized and 7-ton ingots were uphill teemed. Billets with a square section of 100×100 mm were rolled with the use of conventional methods. As part of the second procedure, steel was also melted in a 140-ton basic arc furnace. After tapping into a ladle, steel was additionally refined with argon. Gas was introduced through a porous brick, and the procedure was completed in 8-10 minutes. Steel was poured into moulds, and billets were rolled similarly as in the first method. In the third process, steel was melted in a 100-ton oxygen converter and deoxidized by vacuum. Steel was cast continuously and square 100x100 mm billets were rolled. Billet samples were collected to determine:

– chemical composition. The content of alloy constituents was estimated with the use of LECO analyzers, an AFL FICA 31000 quantometer and conventional analytical methods;
– relative volume of non-metallic inclusions with the use of the extraction method,
– dimensions of impurities by inspecting metallographic specimens with the use of a Quantimet 720 video inspection microscope under 400x magnification. It was determined for a larger boundary value of 2 μm.

The number of particles range 2 μm and smaller was the difference between the number of all inclusions determined by chemical extraction and the number of inclusions measured by video method.

Analytical calculations were performed on the assumption that the quotient of the number of particles on the surface divided by the area of that surface was equal to the quotient of the number of particles in volume divided by that volume [20].

It in aim of qualification of fatigue proprieties from every melting was taken 51 sections. The sections possessing the shapes of cylinder about diameter 10 mm. Their main axises be directed to direction of plastic processing simultaneously. It thermal processing was subjected was in aim of differentiation of building of structural sample [20]. It depended on hardening from austenitizing by 30 minutes in temperature 880°C after which it had followed quenching in water, for what was applied drawing. Tempering depended on warming by 120 minutes material in temperature 200, 300, 400, 500 or 600°C and cooling down on air.

The average chemical composition of the analyzed steel is presented in Table 1.

TABLE 1
Average chemical composition of the analyzed steel

C	Mn	Si	P	S	Cr	Ni	Mo	Cu	B
0.24	1.19	0.25	0.02	0.013	0.51	0.49	0,24	0.11	0.003

Fatigue strength was determined for all heats. Heat treatment was applied to evaluate the effect of hardening on the fatigue properties of the analyzed material, subject to the volume of fine non-metallic inclusions. During heat treatment, steel sections were hardened and tempered at a temperature of 200, 300, 400, 500 and 600°C. The application of various heat treatment parameters led to the formation of different microstructures responsible for steel hardness values in the following range from 271 to 457 HV.

Examination was realized on calling out to rotatory curving machine about frequency of pendulum cycles: 6000 periods on minute. For basis was accepted was on fatigue defining endurance level 10^7 cycles. The level of fatigue-inducing load was adapted to the strength properties of steel. Maximum load was set at:

– for steel tempered at a temperature of 200°C - 650 MPa,
– for steel tempered at a temperature of 300°C - 500°C - 600 MPa,
– for steel tempered at a temperature of 600°C - 540 MPa.

During the test, the applied load was gradually reduced in steps of 40 MPa (to support the determinations within the endurance limit). Load values were selected to produce 10^4-10^6 cycles characterizing endurance limits [1,4].

The general form of the mathematical model is presented by equation (1)

$$z_{go\,(temp.\,tempered)} = aV_0 + b \tag{1}$$

where:

z_{go} – rotating bending fatigue strength [MPa]

V_0 – relative volume of non-metallic inclusions range 2 μm and smaller [vol. %].

a, b – coefficients of the equation

The significance of correlation coefficients r was determined on the basis of the critical value of the Student's t-distribution for a significance level α =0.05 and the number of degrees of freedom f = n-2 by formula (2).

$$t = \frac{r}{\sqrt{\frac{1-r^2}{n-2}}} \tag{2}$$

The values of the diffusion coefficient z_{go} near the regression line were calculated with the use of the below formula (3):

$$\delta = 2s_{zgo}\sqrt{1-r^2} \tag{3}$$

where:

s_{zgo} – standard deviation,

r – correlation coefficient.

3. The results of investigations and their analysis

The microstructure of steel hardened and tempered at 200°C is presented in Fig. 1. Bending fatigue strength of steel hardened and tempered at 200°C in depends of volume of inclusions are presented in Fig. 2, regression equation and correlation coefficients r at (4).

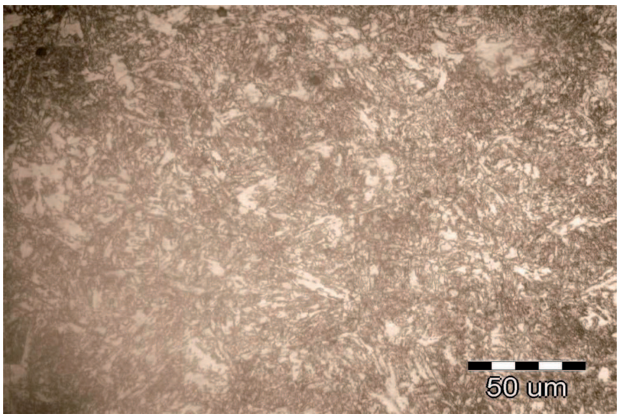

Fig. 1. Microstructure of steel hardened and tempered at 200°C. Tempered martensite. Hardness 457 HV. Mag. 500x

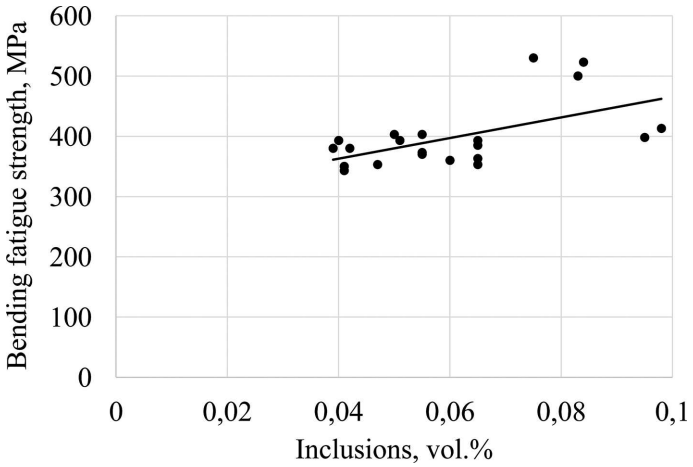

Fig. 2. Bending fatigue strength of steel hardened and tempered at 200°C subject to volume of inclusions

$$z_{go(200)} = 1714.9V_0 + 294.25 \text{ and } r = 0.5696 \quad (4)$$

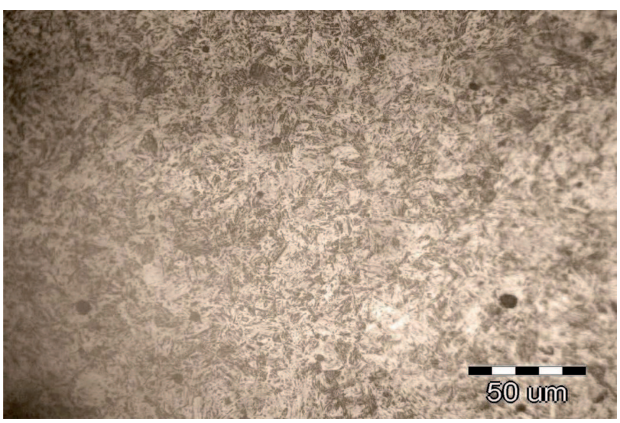

Fig. 3. Microstructure of steel hardened and tempered at 300°C. Tempered martensite with metastable carbides. Hardness 387 HV. Mag. 500x

The microstructure of steel hardened and tempered at 300°C is presented in Fig. 3. Bending fatigue strength of steel hardened and tempered at 300°C in depends of volume of inclusions are presented in Fig. 4, regression equation and correlation coefficients r at (5).

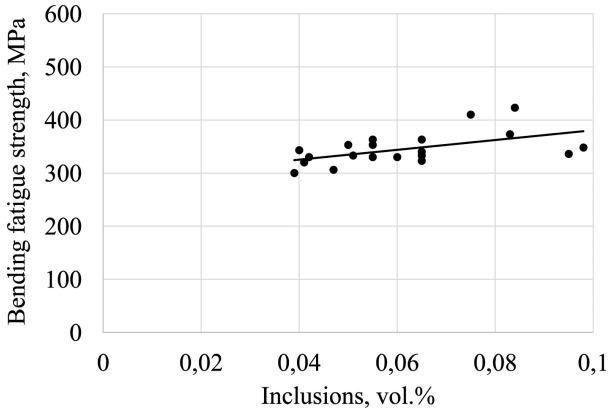

Fig. 4. Bending fatigue strength of steel hardened and tempered at 300°C subject to volume of inclusions

$$z_{go(300)} = 917.66V_0 + 288.75 \text{ and } r = 0.5441 \quad (5)$$

The microstructure of steel hardened and tempered at 400°C is presented in Fig. 5. Bending fatigue strength of steel hardened and tempered at 400°C in depends of volume of inclusions are presented in Fig. 6, regression equation and correlation coefficients r at (6).

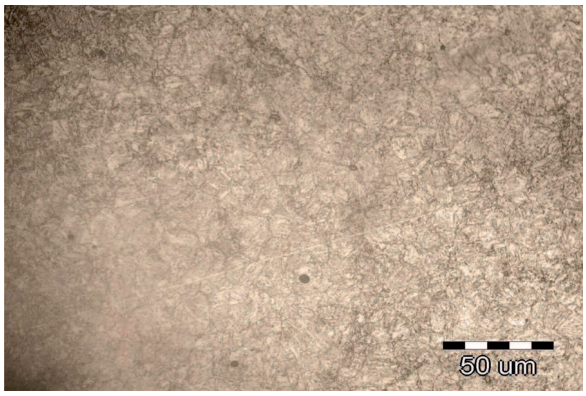

Fig. 5. Microstructure of steel hardened and tempered at 400°C. Tempered martensite with cementite formations coherently bonded with the groundmass. Hardness 370 HV. Mag. 500x

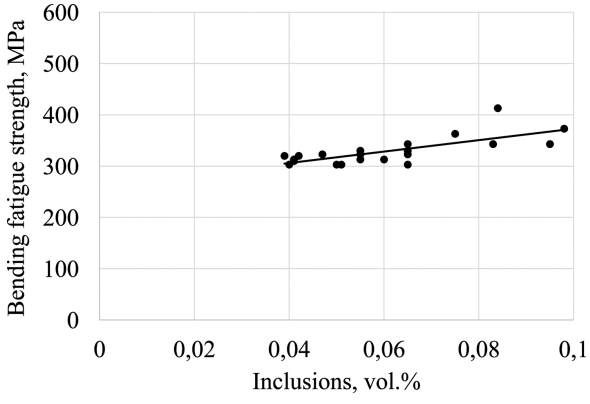

Fig. 6. Bending fatigue strength of steel hardened and tempered at 400°C subject to volume of inclusions

$$z_{go(400)} = 1114.5V_0 + 261.5 \text{ and } r = 0.7322 \quad (6)$$

The microstructure of steel hardened and tempered at 500°C is presented in Fig. 7. Bending fatigue strength of steel hardened and tempered at 500°C in depends of volume of inclusions are presented in Fig. 8, regression equation and correlation coefficients r at (7).

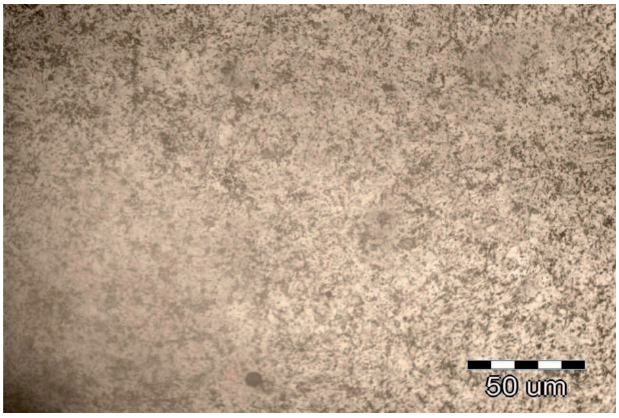

Fig. 7. Microstructure of steel hardened and tempered at 500°C. Sorbit – mixture of ferryt and submicroscopic carbides. Hardness 316 HV. Mag. 500x

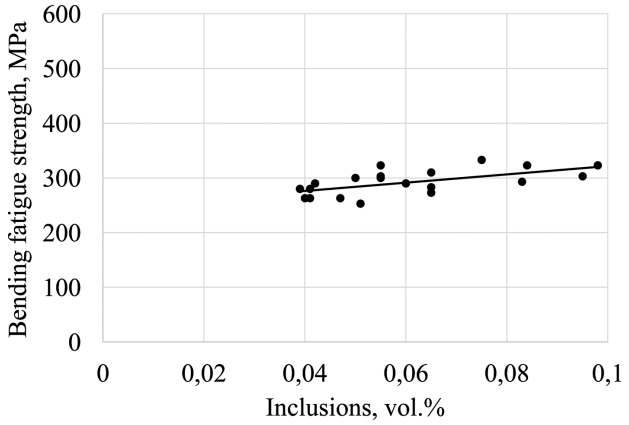

Fig. 8. Bending fatigue strength of steel hardened and tempered at 500°C subject to volume of inclusions

$$z_{go(500)} = 757.23V_0 + 245.69 \text{ and } r = 0.5943 \quad (7)$$

The microstructure of steel hardened and tempered at 600°C is presented in Fig. 9. Bending fatigue strength of steel hardened and tempered at 600°C in depends of volume of inclusions are presented in Fig. 10, regression equation and correlation coefficients r at (8).

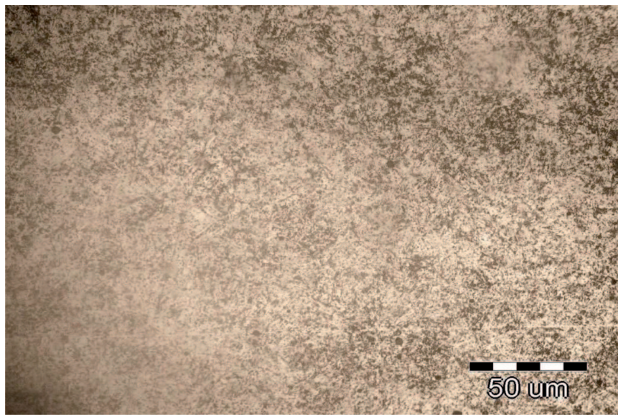

Fig. 9. Microstructure of steel hardened and tempered at 600°C. Globular cementite in ferrite matrix. Hardness 271 HV. Mag. 500x

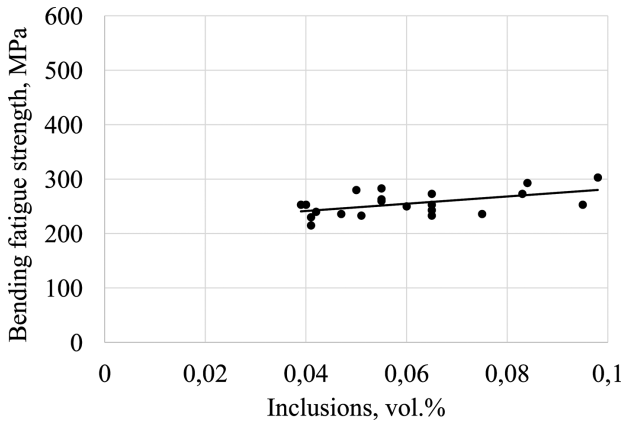

Fig. 10. Bending fatigue strength of steel hardened and tempered at 600°C subject to volume of inclusions

$$z_{go(600)} = 668.43V_0 + 214.59 \text{ and } r = 0.5292 \quad (8)$$

The principal structure of steel is identical for the remaining two production methods with respective heat treatment variants.

Statistical parameters representing the results of the experiment are presented in Table 2.

TABLE 2
Statistical parameters representing the results of the experiment

t $_{temp.}$, °C	$\bar{z_{go}}$, MPa	s_{zgo}, MPa	$\bar{HV}$	s_{HV}	$\bar{V}_0$, %	s_{Vo}, %
200	398	54.0	418	43.3	0.061	0.018
300	344	30.0	383	28.6		
400	329	27.0	355	25.2		
500	292	22.8	327	17.3		
600	257	22.8	280	27.5		

Parameters representing mathematical models and correlation coefficients are presented in Table 3.

The analysis of coefficients a and b (tab. 3) in regression equations (1) indicates that fatigue strength (parameter b) decreases and the effect of non-metallic inclusions (parameter a) increases with a rise in tempering temperature.

TABLE 3

Parameters representing mathematical models and correlation coefficients

Tempering temperature °C	Regression coefficient a (1)	Regression coefficient b (1)	Correlation coefficient r	Degree of dissipation z_{go} around regression line δ [MPa] (3)	$t_{\alpha=0.05}$ calculated by (2)	$t_{\alpha=0.05}$ from Student's distribution for p=(n-2)
200	1714.9	294.25	0.5696	88.8	3.023	2.093
300	917.66	288.75	0.5441	50.33	2.8236	
400	1114.5	261.5	0.7322	36.78	4.684	
500	757.23	245.69	0.5943	36.67	3.219	
600	668.43	214.59	0.5292	36.69	3.718	

4. Conclusions

The results of the study indicate that fatigue strength, represented by fatigue strength during rotary bending, is correlated with the relative volume of non-metallic inclusions measuring up to 2 μm. The presence of statistically significant correlations was verified by Student's t-test.

Our findings support the conclusion that submicroscopic non-metallic inclusions inhibit the propagation of fatigue cracks.

The higher the tempering temperature, the lower the hardness of steel, and the smaller the dispersion of values around the regression line.

The results of the study indicate that the presence of non-metallic inclusions measuring up to 2 μm increases the magnitude of stress that induces fatigue cracking. The said increase is proportional to the relative volume of inclusions, but the final outcome is also determined by the strength of the metallic groundmass (δ).

Non-metallic inclusions block slip systems, inhibit dislocation activities and the formation of microcracks, thus increasing the stress required for the propagation of fatigue cracking.

REFERENCES

[1] J. Szala, Ocena trwałości zmęczeniowej elementów maszyn w warunkach obciążeń losowych i programowych. Bydgoszcz Akademia Techniczno-Rolnicza (1980) (in Polish).

[2] D. Spriestersbach, P. Grad, E. Kerscher, Influence of different non-metallic inclusion types on the crack initiation in high-strength steels in the VHCF regime. Intern. J. of Fatig. **64**, 114-120 (2014).

[3] T. Lipiński, A. Wach, The effect of the production process of medium-carbon steel on fatigue strength, Arch. of Foundry Eng. **10**, 2, 79-82 (2010).

[4] S. Kocańda, Zmęczeniowe pękanie metali, (1985) WNT Warsaw (in Polish).

[5] T. Lipiński, A. Wach, The effect of out-of-furnace treatment on the properties of high-grade medium-caborn structural steel, Arch. of Foundry Eng. **10**, 93-96 (2009).

[6] T. Himemiya, W. Wołczyński, Prediction of Solidification Path and Solute Redistribution of an Iron-based Multi-component Alloy Considering Solute Diffusion in the Solid Materials. Transactions of the Japan Institute of Metals **43**, 2890-2896 (2002).

[7] W. Wołczyński, Concentration Micro-Field for Lamellar Eutectic Growth. Defect and Diffusion Forum **272**, 123-138 (2007).

[8] D. Kalisz, Interaction of Non-Metallic Inclusion Particles With Advancing Solidification Front. Arch. of Metallurgy and Mat. **59**, 2 (2014).

[9] Y. Murakami, Metal fatigue: Effects of small defects and inclusions. Amsterdam Elsevier (2002).

[10] T. Lis, Modification of non-metallic dispersion phase in steel, Met. and Foundry Eng. **1**, 28, 29-45 (2002).

[11] T. Lipiński, A. Wach, The Share of Non-Metallic Inclusions in High-Grade Steel for Machine Parts, Arch. of Foundry Eng. **10**, 4, 45-48 (2010).

[12] V.S. Gulyakov, A.S. Vusikhis, D.Z. Kudinov, Nonmetallic Oxide Inclusions and Oxygen in the Vacuum_Jet Refining of Steel. Steel in Translation **42**, 11, 781-783 (2012).

[13] T. Lipiński, A. Wach, Dimensional Structure of Non-Metallic Inclusions in High-Grade Medium Carbon Steel Melted in an Electric Furnace and Subjected to Desulfurization. Solid State Phenomena **223**, 46-53 (2015).

[14] T. Lipiński, A. Wach, Influence of Outside Furnace Treatment on Purity Medium Carbon Steel. 23rd International Conference on Metallurgy and Materials METAL 2014. TANGER Ltd., Ostrava. Conference proceedings 738-743 (2014).

[15] S. Beretta, Y. Murakami, Largest-Extreme-Value Distribution Analysis of Multiple Inclusion Types in Determining Steel Cleanliness. Met. And Mat. Trans. B **32B**, 517-523 (2001).

[16] J.M. Zhanga, J.F. Zhang, Z.G. Yang, G.Y. Li, G. Yao, S.X. Li, W.J. Hui, Y.Q. Weng, Estimation of maximum inclusion size and fatigue strength in high-strength ADF1 steel. Mat. Sc and Eng. A **394**, 126-131 (2005).

[17] S. Hong, S.Y. Shin, H.S. Kim, S. Lee, S. Kim, K. Chin, N.J. Kim, Effects of Inclusions on Delayed Fracture Properties of Three Twinning Induced Plasticity (TWIP) Steels. Met. And Mat. Trans. A, 776-786 (2013).

[18] Y. Zeng, H. Fan, X. Xie, Effects of the shape and size of rectangular inclusions on the fatigue cracking behavior of ultra-high strength steels. Int. J. of Minerals, Met. and Mat. **20**, 4, 360-364 (2013).

[19] M.G. Hebsur, K.P. Abracham, V.V. Prasad, Effect of electroslag refining on the fracture toughness and fatigue crack propagation rates in heat treatment AISI 4340 steel. Eng. Fract. Mech. **13**, 4, 851-864 (1980).

[20] J. Ryś, Stereology of materials. FOTOBIT DESIGN, Krakow (1995) (in Polish).

Received: 20 February 2014.